

Computer-Aided Planning and Reconstruction of Cranial 3D Implants

Markus Gall, Xing Li, Xiaojun Chen, Dieter Schmalstieg, Jan Egger

Abstract— In this contribution, a prototype for semi-automatic computer-aided planning and reconstruction of cranial 3D Implants is presented. The software prototype guides the user through the workflow, beginning with loading and mirroring the patient's head to obtain an initial curvature of the cranial implant. However, naïve mirroring is not sufficient for an implant, because human heads are in general too asymmetric. Thus, the user can perform Laplacian smoothing, followed by Delaunay triangulation, for generating an aesthetic looking and well-fitting implant. Finally, our software prototype allows to save the designed 3D model of the implant as a STL-file for 3D printing. The 3D printed implant can be used for further pre-interventional planning or even as the final implant for the patient. In summary, our findings show that a customized MeVisLab prototype can be an alternative to complex commercial planning software, which may not be available in a clinic.

I. INTRODUCTION

Cranioplasty is among the oldest surgical procedures and trauma, infections, tumors and compression caused by brain edema are some of the reasons for the removal of bone [1]. However, the reconstruction becomes difficult, if the defect is large and located in the fronto-orbital region, which is an area requiring aesthetic considerations. Thus, good preoperative evaluation, surgical planning and preparation, and accurate restoration of the anatomical contours are mandatory for a satisfactory outcome [2]. Computer-aided planning of cranial 3D implants has gained importance during the last decade due to the limited time in clinical routine, especially in emergency cases and to avoid complications [3]. But, state-of-the-art techniques are still quiet time consuming due to a low level approach. Generally speaking, CT scans are used to design an implant, often using non-medical software, which is not really appropriate. As a result, neurosurgeons spend hours with tedious low level operations on polygonal meshes for designing a satisfactory 3D implant. Commercial implant modeling software [4], like MIMICS, Biobuild or 3D-Doctor, is not always available, but if it is, using such software can be very complex.

M. G. is with the Institute for Computer Graphics and Vision, Graz University of Technology, Austria (e-mail: gall@student.tugraz.at).

X. L. is with the School of Mechanical Engineering, Shanghai Jiao Tong University, Shanghai, China (e-mail: lihouxing@yeah.net).

X. C. is with the School of Mechanical Engineering, Shanghai Jiao Tong University, Shanghai, China (e-mail: xiaojunchen@sjtu.edu.cn).

D. S. is with the Institute for Computer Graphics and Vision, Graz University of Technology, Austria (e-mail: schmalstieg@tugraz.at).

J. E. is with the Institute for Computer Graphics and Vision, Graz University of Technology, Austria and BioTechMed-Graz, Austria (phone: +43 316 873 5076; fax: +43 316 873 5050; e-mail: egger@tugraz.at).

In this paper, an alternative software allowing fast, semi-automatic planning of cranial 3D implants under MeVisLab [5], [6] is presented. Overall, the introduced method uses non-defected areas of the patient's skull as a template for generating an aesthetic looking and well-fitting implant. This is accomplished by mirroring the skull itself and fitting it – at least partly – manually into the defected area. By further marking the defect's boundaries and the surface of the mirrored template in the defected area, the implants shape is defined. Similar methods have been proposed before [7], however our approach enhances the template with automatic application of Laplacian smoothing [8] and Delaunay triangulation [9], giving the implant a better fitting shape.

Others working in the area of computer-aided cranial implant design are Lee et al. [10], who present a custom implant design case for an 8-year-old boy with a large cranial defect. The raw cranial CT data of the patient was translated into a stereolithography format using a computer-aided design/computer-aided manufacturing (CAD/CAM) interface software. However, they do not state which CAD/CAM software, they used or describe it in detail. Van der Meer et al. [11] demonstrate the digital planning of cranial implants for the reconstruction of defects in the skull. The time-consuming workflow includes the usage of a generic industrial software which provides automated procedures and functions like “fill holes” and “curvature-based filling”, which have been used to design the implant. Chulvi et al. [12] introduce the automated design of customized implants by linking two computer prototypes. The core of the model is the Knowledge Based System technology, which is able to store and manage medical data, as well as designer knowledge, in order to use this information in the implant design process. The research is based on the previous study of existing software, like MIMICS, 3D Slicer [13]-[15], ImLib3D, MITK, OsiriX and the Visualization Toolkit. However, to the best of our knowledge, there is no work that has studied the computer-aided planning of cranial 3D implants with MeVisLab.

The paper is organized as follows. Section II presents the details of the proposed algorithm. Section III discusses the results of our experiments. Section IV concludes the paper and outlines areas for future research.

II. MATERIAL AND METHODS

A. Data Acquisition

Scans of patients with cranial defects, provided by the co-authors Xing Li and Xiaojun Chen in STL-file format were used for planning the cranial implants. The defects range from

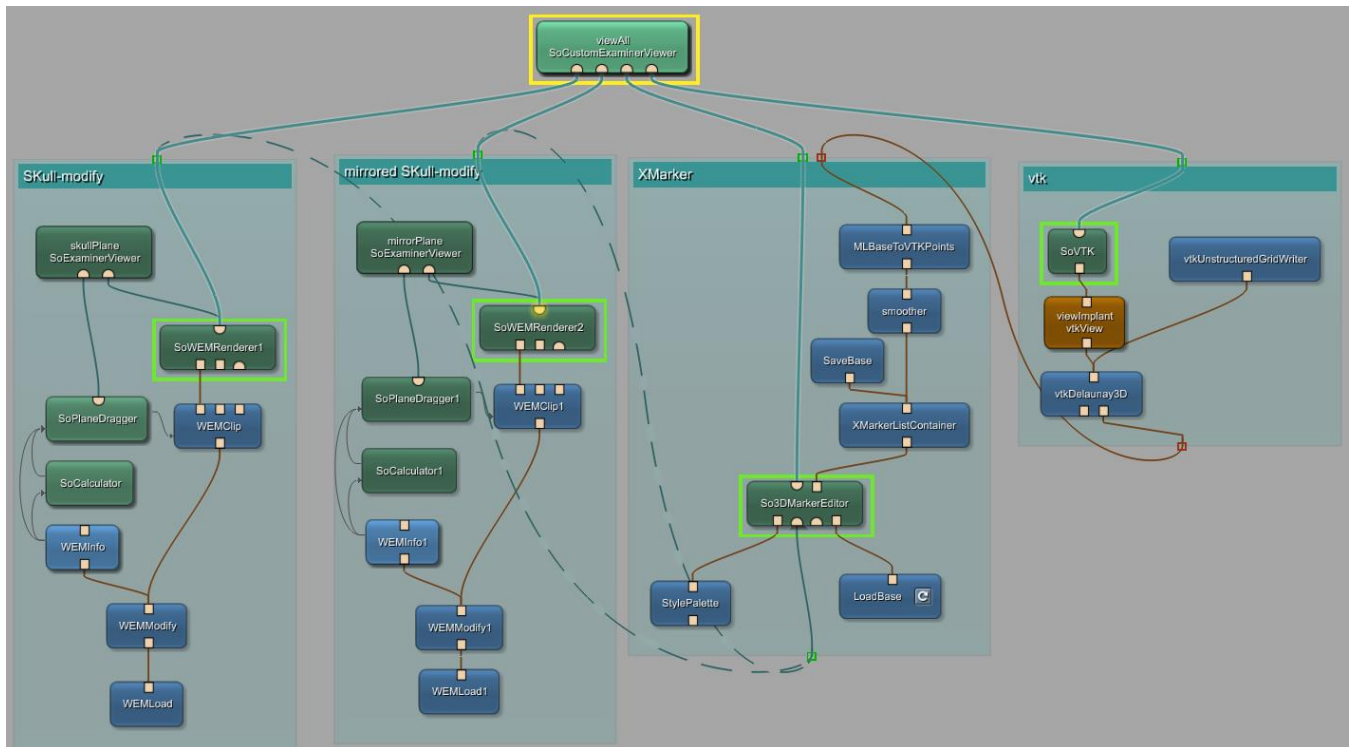


Fig. 1. Network generated in MeVisLab, dashed lines indicate alternate use depending on where the markers are set (original or mirrored object/skull), separated in four big groups: left – loading and modifying original object, middle/left – loading and modifying mirrored object/skull including mirroring, middle/right – performing marker operations like setting, smoothing, etc., right – vtk environment including Delaunay triangulation.

bigger affected areas to smaller ones on several sites. All data sets have been selected retrospectively and anonymized by removing facial characteristics using cutting planes. Furthermore, the cranial defect datasets are freely available online (please cite this paper if you use these in your work): https://www.researchgate.net/publication/303371734_Cranial_Defect_Datasets

B. Software

As cranial implant planning software, a custom data-flow network was set up under MeVisLab (medical image processing and scientific visualization, www.mevislab.de). MeVisLab is a software framework allowing medical image processing and visualization, which has been used for a variety of applications, like centerline extraction [16], stent simulation [17]–[21], boundary estimation of fiber bundles [22] in the brain [23]–[25], Endoleak detection [26], [27] of aortic aneurysms [28] or various segmentation tasks [29]–[42]. The software can combine a wide variety of existing modules, such as loading, processing and visualizing of medical image data, into a dataflow network, and can be extended in C++. In Figure 1, the overall network of our application is shown, where each block represents a module. Different colors represent types of modules: Blue stands for ML modules, which process large voxel datasets. Green marks Open Inventor modules, working with 3D scene graphs. Brown modules are Macro combining other module types. Modules can be concatenated with two types of connections: Undirected lines represent data flow and directed indicate a parameter connection. Data connections

require outputs and input of the same type - squares for base objects (data structures), triangles for ML images and semi-circles for Inventor scenes.

C. Processing Pipeline

We use the healthy side of the cranium as a template for the implant construction. Therefore, the patient dataset is loaded twice, one of the copies is mirrored (Figure 1. middle/left group). However, if the defect is located near the center of the cranial bone, mirroring can lead to an unsatisfying result. In such cases a standard geometrical shape, like a sphere, may be used instead of the mirrored skull. In addition, it is necessary to have a view from the outside as well as from the inside onto the defected area for the planning process. Thus, we created a module network generating a cutting plane for both the original and the mirrored skull (Figure 1. SoPlaneDraggers), enabling the user to cut the object with an arbitrary 3D plane. Next, markers are set manually, beginning with so-called edge markers on the defective border of the original skull. Afterwards, we set the surface markers, which fit the mirrored object into the defect area. This is done for both sides, the inside and the outside edges and surfaces, to define the shape of the implant (Figure 1. middle/right group). It is important to distinguish between the four types of markers (inside, outside, edge and surface) for further smoothing. The list of markers serves as input for the triangulation module. This module uses the markers to automatically generate a triangular mesh by using Delaunay triangulation.

Due to the asymmetry of the human skull, rough edges may be present in the generated mesh, since the mirrored object is just a template and will never fit perfectly into the defective area. Therefore, the triangulated mesh can be enhanced by the user via Laplacian smoothing (Figure 1. smoother module), which is applied automatically according to the user set parameters.

D. Smoother Module

A ML-module was set up using one input, one output and two field-variables serving as user input. The x-parameter sets up the radius in which a neighbor node may lie, and the y-parameter defines the weights of the border nodes. The surrounding structure is set up automatically. Using a list of markers as input, the algorithm calculates a new position for each node based on Laplacian smoothing:

$$\bar{x}_i = \frac{1}{N} \sum_{j=1}^N \bar{x}_j \quad (1)$$

In equation 1, N is the number of adjacent nodes to node i in the given radius, set by the x parameter; x_j is the position of the j^{th} adjacent node, and x_i is the new position for node i . We introduce two improvements over basic Laplacian smoothing: First, we use the x -parameter to restrict markers to a user-defined radius. Second, border markers are set as immutable markers, which cannot be moved in the calculation, since they are already placed on the border. By applying a weight to these immutable markers, they constrain the calculations.

E. Smoother Algorithm

Finally, in Figure 2, the overall flowchart of the main smoothing algorithm is shown. It starts with accessing all markers of the input marker list and ends with the calculation of the new and smoothed position for a current node.

III. RESULTS

The overall planning time for a sufficient cranial 3D implant could be reduced to less than thirty minutes for the most cases. In contrast, our clinical partners who shift vertex per vertex of a geometrical form into position using non-commercial but unappropriated software like the 3D computer graphics software Blender, reported a planning time of three hours. Skull mirroring, marker setting and the

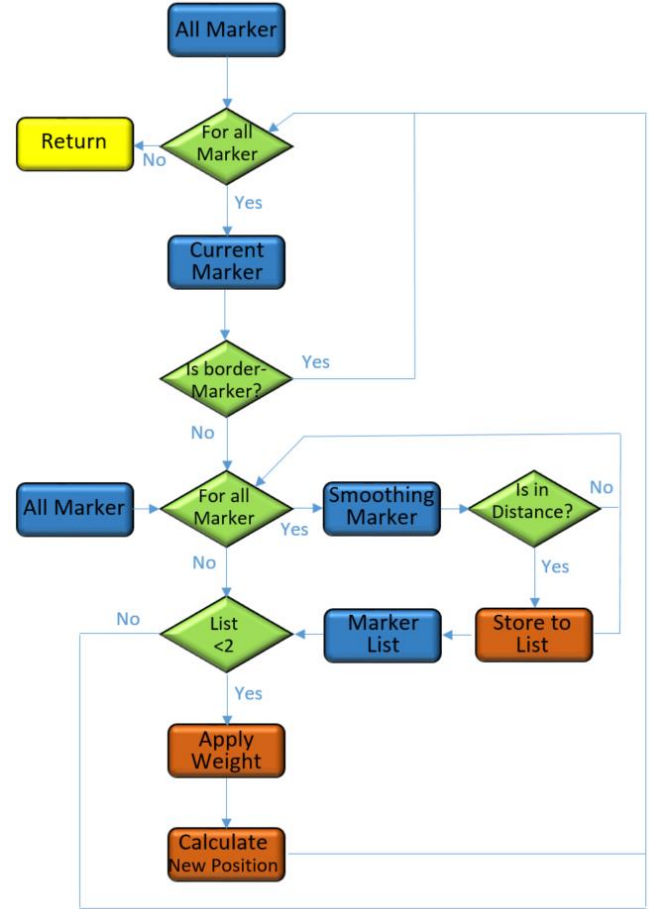


Fig. 2. Flowchart of the smoothing algorithm based on the C++ code where blue boxes are object types, green diamonds represent test expression and orange boxes show processing steps.

smoothing was integrated into a user-friendly planning prototype, which was found easy to use and much faster than the non-medical modelling software applications used by our clinical partners. The planning of a 3D implant with our prototype took a new user less than thirty minutes, while the first author was even able to obtain a similar result in about twelve minutes.

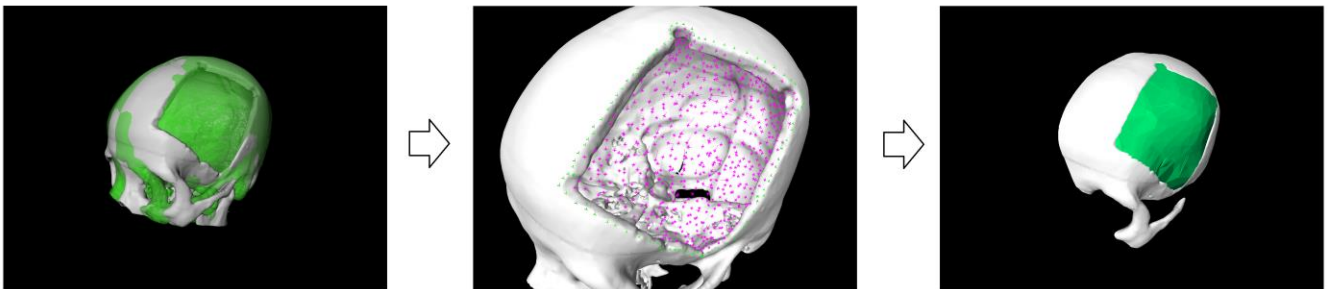


Fig. 3. Stepwise result during the implant generation process in a clinical case with a cranial defect on the left side. Left: Original skull (white) overlapped with the mirrored one (green); Middle: Set markers, border markers in green and surface markers in magenta; Right: Final and smoothed implant (green).

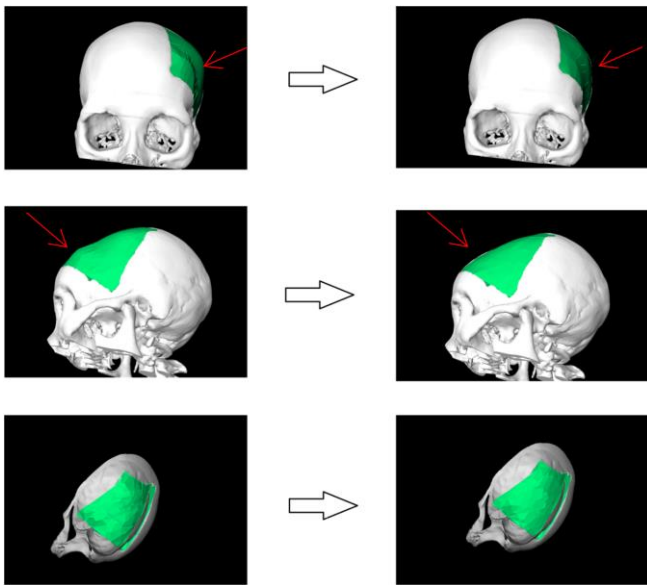


Fig. 4. Result of an unsmoothed (left) and smoothed (right) clinical case with a large cranial defect on the left side. Perceptible is the clear improvement of the surface indicated through the red arrow and the overall result showing a well-fitting and aesthetic looking implant.

Figure 3. shows the results during the three big steps of the implant generation process of a clinical case with a large cranial defect on the left side. In Figure 4. the different results, smoothed and unsmoothed of the same case are investigated. In general, the outcomes show a well-fitting 3D implant on the outer as well as on the inner surface. However, the result of an additional Laplacian smoothing is shown on the right side (red arrow). An additionally tweaking on the vertex level is not necessary, because markers can directly be placed on existing surfaces (note: single markers may be manipulated individually as fallback option). Further, in Figure 5. another clinical, more complex, case is shown. Summarized, the proposed software tool enables surgeons to generate a well-fitting implant which is able to be generated within several minutes, also improving the user’s experience and reducing time consumption, compared to the other methods. Yet, the software was not tested in clinical trials but with the mentioned advantages the tool could be an alternative to commercial software not available at a clinic.

IV. CONCLUSIONS

In this publication, the semi-automatic planning of cranial 3D Implants under MeVisLab has been introduced. Therefore, we presented a MeVisLab prototype consisting of a customized data-flow network. As a result, we demonstrated that MeVisLab could be an alternative to complex commercial planning software which may also not be available in a clinic. The software prototype guides the user through the workflow beginning with loading and mirroring the patients head for an initial curvature of the cranial implant. However, pure mirroring is not sufficient for an implant, because human heads are in general too asymmetric. Thus, the user can perform afterwards Laplacian smoothing, followed by Delaunay triangulation for generating an aesthetic looking and well-fitting implant. Finally, our software prototype allows to save the designed 3D model of the implant as a STL-file for

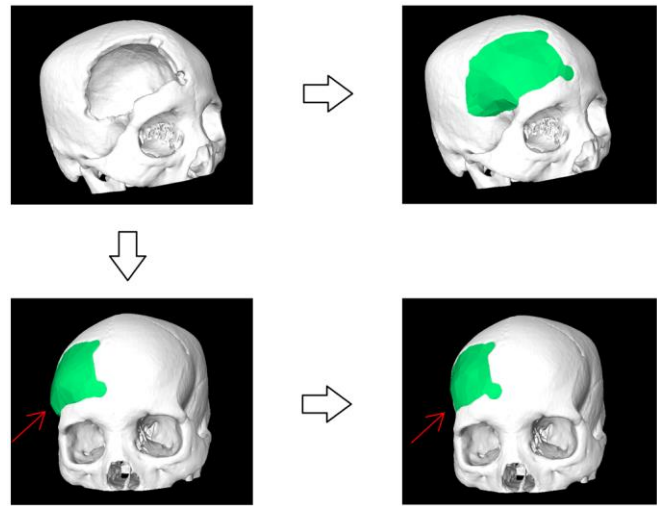


Fig. 5. Result of a clinical case with a large and more complex cranial defect on right-front side (upper-left). Due to the complex form the unsmoothed implant (lower-left) results in a well-fitting but not aesthetic looking result (indicated with the red arrow). However, applying the smoothing algorithm results in a more suitable form (right side).

3D printing. The 3D printed implant can be used for further pre-interventional planning or even as the real implant for the patient [43]. In conclusion, the achieved highlights of this publication are:

- Successful planning and reconstruction of cranial 3D implants under MeVisLab;
- Skull mirroring for an initial curvature of the implant for the defect restoration;
- Additional interactive smoothing and triangulation for an aesthetic looking and well-fitting implant;
- Evaluation with real patient CT data from the clinical routine;
- Exporting of the 3D implant as STL-file for 3D printing.

There are several areas for future work, for example a comparison with commercial and open-source [1] software.

ACKNOWLEDGMENT

The work received funding from the European Union (EU) in FP7: Clinical Intervention Modelling, Planning and Proof for Ablation Cancer Treatment (ClinicIMPACT, grant agreement no. 610886). Dr. Xiaojun Chen receives support from Natural Science Foundation of China (Grant No.: 81511130089) and Foundation of Science and Technology Commission of Shanghai Municipality (Grant No.: 14441901002, 15510722200). DDr. Jan Egger receives funding from BioTechMed-Graz (“*Hardware accelerated intelligent medical imaging*”). A tutorial video demonstrating the cranial implant planning can be found under the YouTube channel: <https://www.youtube.com/c/JanEgger/videos> Cranial defect datasets are freely available online (please cite this paper if you use these in your work): https://www.researchgate.net/publication/303371734_Cranial_Defect_Datasets

REFERENCES

- [1] M. Dujovny, et al. "Cranioplasty: cosmetic or therapeutic?," *Surg Neurol.* 47(3):238–41, 1997.
- [2] L. J. Lo, et al. "Computer-aided reconstruction of traumatic fronto-orbital osseous defects: aesthetic considerations," *Chang Gung Med J.* 27(4):283–91, 2004.
- [3] L. R. Williams, K. F. Fan, R. P. Bentley, "Custom-made titanium cranioplasty: early and late complications of 151 cranioplasties and review of the literature," *Int J Oral Maxillofac Surg.* 2015 May; 44(5):599–608. doi: 10.1016/j.ijom.2014.09.006. Epub 2014 Dec 5.
- [4] J. Parthasarathy. "3D modeling, custom implants and its future perspectives in craniofacial surgery," *Ann Maxillofac Surg.* 4(1): 9–18, 2014.
- [5] J. Egger, et al., "Integration of the OpenIGTLink Network Protocol for image-guided therapy with the medical platform MeVisLab," *Int J Med Robot,* 8(3):282–90, 2012.
- [6] J. Egger, "Image-guided therapy system for interstitial gynecologic brachytherapy in a multimodality operating suite," *SpringerPlus,* 2:395, 2013.
- [7] X. Li, et al., "Symmetry and template guided completion of damaged skulls," *Computers & Graphics* 35, 885–893, 2011.
- [8] N. Amenta, et al., "Optimal Point Placement for Mesh Smoothing," *Journal of Algorithms* 30, 302–322, 1999.
- [9] M. Gopi, et al., "Surface reconstruction based on lower dimensional localized delaunay triangulation," *Computer Graphics Forum,* 19(3):467–478, 2000.
- [10] M. Y. Lee, C. C. Chang, C. C. Lin, L. J. Lo, Y. R. Chen, "Custom implant design for patients with cranial defects," *IEEE Eng Med Biol Mag.* 21(2):38–44, 2002.
- [11] W. J. van der Meer, R. R. Bos, A. Vissink, A. Visser, "Digital planning of cranial implants," *Br J Oral Maxillofac Surg.* 2013 Jul; 51(5):450–2. doi: 10.1016/j.bjoms.2012.11.012. Epub 2012 Dec 23.
- [12] V. Chulvi, D. Cebrian-Tarrasón, Á. Sancho, R. Vidal. "Automated design of customized implants," *Revista Facultad de Ingeniería Universidad de Antioquia* 68, pp. 95–103, 2013.
- [13] J. Egger, et al., "Pituitary Adenoma Volumetry with 3D Slicer," *PLoS ONE* 7, e51788, 2012.
- [14] J. Egger, et al., "GBM Volumetry using the 3D Slicer Medical Image Computing Platform," *Sci Rep.* 3, 1364, 2013.
- [15] X. Chen, et al., "Development of an Open Source Software Module for Enhanced Visualization during MR-Guided Interstitial Gynecologic Brachytherapy," *SpringerPlus,* 3:167, 2014.
- [16] J. Egger, et al., "A Fast Vessel Centerline Extraction Algorithm for Catheter Simulation," *CBMS,* 177-182, IEEE Press, June 2007.
- [17] J. Egger, et al., "Simulation of Bifurcated Stent Grafts to Treat Abdominal Aortic Aneurysms (AAA)," *SPIE,* 6509, 1–6, 2007.
- [18] J. Egger, et al., "Modeling and Visualization Techniques for Virtual Stenting of Aneurysms and Stenoses," *Comput Med Imaging Graph.,* 36(3):183-203, 2012.
- [19] J. Egger, et al., "Preoperative Measurement of Aneurysms and Stenosis and Stent-Simulation for Endovascular Treatment," *ISBI,* 392-5, 2007.
- [20] J. Egger, et al., "Aorta Segmentation for Stent Simulation," *Cardiovascular Interventional Imaging and Biophysical Modelling Workshop, MICCAI,* pages 1-10, 2009.
- [21] J. Egger, et al., "Fast Self-Collision Detection and Simulation of Bifurcated Stents to Treat Abdominal Aortic Aneurysms (AAA)," *29th Annual International Conference of the IEEE Engineering in Medicine and Biology Society,* Lyon, France, 6231-6234, IEEE Press, 2007.
- [22] D. Kuhnt, et al., "Fiber tractography based on diffusion tensor imaging (DTI) compared with High Angular Resolution Diffusion Imaging (HARDI) with compressed sensing (CS) – initial experience and clinical impact," *Neurosurgery,* Volume 72, pp. A165-A175, 2013.
- [23] M. H. A. Bauer, et al., "A fast and robust graph-based approach for boundary estimation of fiber bundles relying on fractional anisotropy maps," *20th International Conference on Pattern Recognition (ICPR),* Istanbul, Turkey. IEEE Computer Society, 4016-4019, 2010.
- [24] J. Klein, et al., "On the Reliability of Diffusion Neuroimaging," *Neuroimaging, Sciyo,* 1-24, ISBN 978-953-307-127-5, 2010.
- [25] M. H. A. Bauer, et al., "Boundary Estimation of Fiber Bundles derived from Diffusion Tensor Images," *Int J CARS,* 6(1):1–11, 2011.
- [26] J. Lu, et al., "Detection and Visualization of Endoleaks in CT Data for Monitoring of Thoracic and Abdominal Aortic Aneurysm Stents," *SPIE Med Img* 6918, 69181F(1–7), 2008.
- [27] J. Lu, et al., "Segmentation and Visualization of Lumen and Thrombus of Thoracic Aortic Aneurysm," *CURAC,* 251-254, 2007.
- [28] R. D. Renapurkar, et al., "Aortic volume as an indicator of disease progression in patients with untreated infrarenal abdominal aneurysm," *Eur J Radiol.,* 81(2):e87-93, 2011.
- [29] J. Egger, et al., "Nugget-Cut: A Segmentation Scheme for Spherically and Elliptically-Shaped 3D Objects," *DAGM* 6376, 383-392, 2010.
- [30] J. Egger, et al., "Square-Cut: A Segmentation Algorithm on the Basis of a Rectangle Shape," *PLoS One,* 7(2):e31064, 2012.
- [31] J. Egger, et al., "Interactive Volumetry of Liver Ablation Zones," *Sci Rep.,* Nature Publishing Group (NPG), 5: 15373, 2015.
- [32] K. Greiner, et al., "Segmentation of Aortic Aneurysms in CTA Images with the Statistic Approach of the Active Appearance Models," *Proceedings of Bildverarbeitung für die Medizin (BVM),* Berlin, Germany, Springer Press, pp. 51–55, 2008.
- [33] J. Egger, et al., "Interactive-Cut: Real-Time Feedback Segmentation for Translational Research," *Comp Med Imaging Graph* 38, 285–95, 2014.
- [34] J. Egger, et al., "A Flexible Semi-Automatic Approach for Glioblastoma multiforme Segmentation," *Biosignal,* ID:060:1-4, 2010.
- [35] R. Schwarzenberg, et al., "A Cube-Based Approach to Segment Vertebrae in MRI-Acquisitions," *BVM,* Springer, 69–74, 2013.
- [36] J. Egger, et al., "Pituitary Adenoma Segmentation," *Proc. of Inter. Biosignal Processing Conf.,* Paper-ID 061, 1-4, 2010.
- [37] J. Egger, et al., "A Comparison of Two Human Brain Tumor Segmentation Methods for MRI Data," *RBC,* 40-44, 2010.
- [38] J. Egger, "Refinement-Cut: User-Guided Segmentation Algorithm for Translational Science," *Sci. Rep.,* 4, 5164, 2014.
- [39] R. Schwarzenberg, et al., "Cube-Cut: Vertebral Body Segmentation in MRI-Data through Cubic-Shaped Divergences," *PLoS One,* 9(4):e93389, 2014.
- [40] J. Egger, et al., "Template-Cut: A Pattern-Based Segmentation Paradigm," *Sci Rep.,* Nature Publishing Group (NPG), 2:420, 2012.
- [41] T. Lüddemann, et al., "Interactive and scale invariant segmentation of the rectum/sigmoid via user-defined templates," *SPIE* 9784, 1–6, 2016.
- [42] J. Egger, "PCG-Cut: Graph Driven Segmentation of the Prostate Central Gland," *PLoS One* 8, e76645, 2013.
- [43] X. Chen, et al., "A semi-automatic computer-aided method for surgical template design," *Sci. Rep.* 6, 20280, Nature Publishing Group (NPG), 2016.
- [44] X. Li, et al., "A semi-automatic implant design method for cranial defect restoration," *Computer Assisted Radiology and Surgery,* PO 064, 2016.